Mean-field simulation of metal oxide antiferromagnetic films and multilayers

M. Charilaou and F. Hellman

Mean-field simulation of metal oxide antiferromagnetic films and multilayers

M. Charilaou* and F. Hellman

Department of Physics, University of California,

Berkeley, California 94720-7300, USA

(Dated: May 10, 2013)

Abstract

In this work the magnetization in antiferromagnetic thin films and multilayers with inter-layer exchange coupling is simulated using mean-field approximation. Transition-metal oxide antiferromagnets are modeled as multi-plane magnetic systems with 1 to 11 planes and the magnetization M is calculated as a function of temperature T. The antiferromagnetic films exhibit ferromagnetism when the number of monolayers is odd, i.e., when there is an uncompensated plane, but the net magnetization is lower than that of any single uncompensated plane due to cancellations and finite-size effects. With increasing film thickness the Néel temperature increases monotonically and the magnetic moment near the surface is reduced compared to that of the core, changing the form of the $M(T)$ curve. When antiferromagnetic films are exchange coupled to each other, as in a multilayer with a non-magnetic intervening layer, the surface magnetization of each film increases and the ferromagnetism of odd-numbered systems is enhanced. These results are shown to be experimentally testable by comparing magnetometry and neutron diffraction.

I.   INTRODUCTION

The magnetization and ordering temperature of thin magnetic films have been studied extensively because of their technological importance and due to fundamental interest in new phenomena which emerge at the nano-scale. While finite-size effects most often reduce the magnetic properties of thin films, in metallic ferromagnetic (FM) films, with the exception of Ni on Cu, the magnetic moments at the surface or interface are larger than in the bulk[1–5] due to band narrowing at the surface and a large density of states (DOS) at the Fermi level[3]. In contrast, antiferromagnetic (AFM) metal oxide films (MO) have localized magnetic moments and their DOS at the Fermi level is zero, therefore the formation of surface states, and thus the enhancement of surface magnetism, is not expected[6]. This was shown for Heisenberg antiferromagnets, where the ordering temperature increases monotonically with increasing film thickness[7], and the surface magnetization is reduced compared to the film core in the absence of quantum fluctuations[8].

The magnetic properties of oxide antiferromagnetic films have been increasingly investigated[9–12], especially after the discovery of exchange bias[13] and giant magnetoresistance[14]. Oxides of the transition metals Mn, Fe, Co, and Ni are antiferromagnetic with Néel temperatures of[15–18] $T_{\mathrm{N}} \approx 120$ K for MnO, 200 K for FeO, 300 K for CoO, and 520 K for NiO. Below T_{N}, spins are ferromagnetically coupled within (111) planes of the NaCl structure and antiferromagnetically coupled to neighboring planes[17] and, with the exception of FeO, the magnetization lies predominantly inside the (111) plane[17]. This magnetic configuration in MO AFM thin films, in which alternating planes cancel each other out, leads to a dominance of uncompensated spins, which may be coupled to the Néel vector or not, in the measured magnetization of such systems. Recently, this aspect was exploited and it was experimentally shown that AFM multilayers can be used as a source of ferromagnetism, arising from uncompensated magnetization coupled via a lightly doped semiconductor, in a new type of magnetic semiconductor[19]. The findings of that work motivated this theoretical investigation. Identifying the mechanisms which govern the magnetization in such systems is crucial to fully understand and predict the behavior of exchange biased films and exchange-coupled multilayers of magnetic semiconductors with uncompensated AFM films. The magnetization properties in such systems are dominated by finite-size effects which reduce the magnetic moment near the surface, thus generating a magnetization profile as a

40 function of film thickness. While the magnetization profiles in thin ferromagnetic films have
41 been studied extensively[20–23], the effect of finite-size on the magnetization of AFM films is
42 not known.

43   In this work we therefore present a theoretical study of AFM films and multilayers using
44 a simple mean-field model for a metal-oxide in the NaCl structure, where the system consists
45 of ferromagnetically ordered (111) planes which are antiferromagnetically coupled to each
46 other. We chose to use the mean-field method because it is the most suitable approach for
47 the description phase transitions in systems with many sublattices, as in the case of the
48 AFM films, where each atomic plane is treated as a sublattice to obtain the magnetization
49 profile. Our focus lies on the magnetization profile as a function of thickness and its impact
50 on the net magnetization in thin AFM films. While it is intuitive that uncompensated AFM
51 films, i.e., with odd number of atomic planes, exhibit non-zero magnetization, in section III
52 it will be seen that the net magnetization of an uncompensated AFM film is, surprisingly,
53 not equal to the magnetization of any single uncompensated plane.

54 **II.   THEORETICAL MODEL**

55   Let us consider the Hamiltonian of the system, in which spins interact with their nearest
56 neighbors, and with an external field:

$$\mathcal{H} = -\frac{1}{2}\sum_i^N \sum_j^z J_{ij} S_i S_j - h \sum_i^N S_i \ . \tag{1}$$

57   The spin S represents the localized total angular momentum, J_{ij} is the exchange coupling
58 constant between S_i and S_j, and h is the external field. The sum over i runs to the total
59 number of spins N and the sum over j runs to the number of nearest neighbors z of each
60 spin S_i.

61   Considering the sheet-wise ordering of MO inside the (111) planes, we divide the system
62 into alternating planes. In a system with D planes, each containing N_d ions, the first term
63 of the Hamiltonian can be broken down to account for interactions within the same plane d
64 with coordination number z via exchange constant J and interactions with the spins in the
65 neighboring planes with coordination number z^* via an inter-plane exchange constant J^*,
66 which we scale with J, i.e., $J^* = \alpha J$. The Hamiltonian for each plane d then reads:

3

$$\mathcal{H}_d = -\frac{1}{2}\sum_{i}^{N_d}\left[\sum_{j}^{z} J S_{d,i} S_{d,j} + \sum_{j}^{z^*} J^* S_{d,i}\left(S_{d+1,j} + S_{d-1,j}\right)\right]$$
$$- h\sum_{i}^{N_d} S_{d,i}. \tag{2}$$

The Hamiltonian of the entire system is then the sum of all planes: $\mathcal{H} = \mathcal{H}_1 + \ldots + \mathcal{H}_d +$ $\ldots + \mathcal{H}_D$. We simplify the Hamiltonian in Eq. 2 using the Weiss mean-field approximation (MFA), i.e., by introducing the magnetization $m_d = \langle S_d \rangle$ which corresponds to the mean field in the dth plane. The strength of the mean field depends on the number of neighbors, i.e., z and z^*, which in the ABC stacking of (111) planes in the NaCl structure is 6 and 3, respectively. The MFA treatment decouples all the spins and reduces the Hamiltonian to that of a single spin for each plane:

$$\mathcal{H}_d^{\mathrm{MFA}} = \underbrace{\frac{N_d}{2}\left[zJm_d^2 + z^*J^*m_d\left(m_{d+1} + m_{d-1}\right)\right]}_{X_d}$$
$$- \underbrace{\left[zJm_d + h + z^*J^*\left(m_{d+1} + m_{d-1}\right)\right]}_{Y_d}\sum_{i}^{N_d} S_{d,i}\,. \tag{3}$$

The partition function $Z(T)$ and the equation of state for the above Hamiltonian can be obtained after choosing the type of spins. Heisenberg-type spins have $S(S+1)$ possible values and the equation of state for the z projection is the Brillouin function[5], but low-dimensional systems with isotropic exchange exhibit no long-range order[24,25]. In contrast, Ising systems have infinite anisotropy, where Ising-type spins can only take $\pm S$ values and the equation of state is of the form[26,27]:

$$m_d = |S|\tanh\left(|S|\,\beta Y_d\right) = f(m_{d-1}, m_d, m_{d+1})\,, \tag{4}$$

with β the inverse temperature $1/T$, and $|S|$ the absolute spin value which is set to 2, i.e., the value for Co^{+2} spins $(\mu_{\mathrm{Co}^{+2}} \approx 3.8\mu_{\mathrm{B}})$[17]. We choose to use Ising spins in our calculations because CoO behaves more like an Ising system due to its high anisotropy[11,28,29]. Moreover, we scale all the energy contributions, i.e., the temperature T and the external field h with the intra-plane exchange constant J. For the inter-plane exchange we use values of $\alpha = -0.5$, -1.0, and -1.5. While the most common choice for α for CoO would be[30] -2 or -3 , our

4

choice of parameters is directed towards a general description and understanding of this type of AFM system, where the ratio α is the dominant mechanism for finite-size effects, as will be seen below.

For the order parameters we define the net magnetization $M(T)$ of the system and the average absolute value of plane magnetization $|m(T)|$:

$$M(T) = \sum_{d=1}^{D} m_d(T) \tag{5a}$$

$$|m(T)| = \frac{1}{D} \sum_{d=1}^{D} |m_d(T)| \tag{5b}$$

In the discussion each plane magnetization is normalized to 1 at $T = 0$, i.e., divided by $|S| = 2$ which is the magnetic moment per atom in the plane.

Finally, we derive the ordering temperature of a system with $D = 1$ (2 dimensions) and $D = \infty$ (3 dimensions) by expanding Eq. 4 for $h = 0$ and small plane magnetization ($|m| \to 0$). The 2-dimensional system orders at $T_N = zJS^2$, and the 3-dimensional system at $T_N = S^2 J(z + 2\alpha z^*)$. The thickness dependence of the ordering temperature within MFA is[31]:

$$T_N(D) = \frac{S^2 J(z + 2\alpha z^*)}{2} \left(1 + \cos\frac{\pi}{D + 1} \right). \tag{6}$$

Considering the ordering temperature of bulk CoO ($T_N \approx 300$ K), and the coordination numbers $z = 6$ and $z^* = 3$, the exchange constant amounts to $J = 12.5/(1 + \alpha)$ K. This value corresponds to $J = 0.55$ meV (for $\alpha = 1$) which is very close to results from quantum chemical ab-initio calculations for CoO[30] (normalizing their value of 6.5 meV by a factor of 16 due to the use of $|S| = 1/2$ against our $|S| = 2$).

We next expand our model to simulate multilayers of MO films each with D planes, separated by a spacer layer (S) which allows inter-layer exchange interactions. In this context, the inter-layer coupling could be of any nature, including RKKY, dipolar, etc; for an RKKY-type interaction, as suggested in Ref.[19], the spacer needs to have sufficient charge carrier density to facilitate such an interaction, as shown experimentally for CoO/Al-ZnO multilayers, where the RKKY-type IEC is mediated by the electrons of the Al dopants[19]. In that case, the inter-layer coupling J_{IEC} between two surfaces, or sheets of spins, oscillates with the spacer layer thickness, and decays with[32] $J_{IEC} \propto e^{-L_S/\lambda}/L_S^2$, with L_S the thickness

of the spacer layer, and λ the material-specific exchange decay length. We incorporate J_{IEC} in our model by coupling the top and bottom plane of the film with J_{IEC}, as shown in Fig. 1, effectively a type of periodic boundary condition. This corresponds to a stacking of multiple MO films, where the top plane of a film interacts with the bottom plane of the next one and so on. In this context of IEC-induced boundary conditions, when the energy contribution of IEC conflicts with that of J^*, the unit cell of the model needs to be doubled, i.e., to account for the modulation of the exchange constants (see discussion).

In the equation of state this energy contribution has the same form as that of the inter-plane exchange J^*, where the coordination number is set to 1, which means that Y_d (see Eq. 3) in the equation of state for the bottom and the top planes in a film will have the form:

$$Y_1 = zJm_1 + h + z^*J^*m_2 + J_{\mathrm{IEC}}m_D \tag{7a}$$

$$Y_D = zJm_D + h + z^*J^*m_{D-1} + J_{\mathrm{IEC}}m_1 \tag{7b}$$

As with the other energy terms, we scale J_{IEC} with J and try different values which would correspond to a spacer with a few monolayers thickness, assuming a constant decay length λ of 10 monolayers ($J_{\mathrm{IEC}} = 0.2\,J$ and $0.4\,J$).

The equations of state for all planes (Eq. 4) must be solved simultaneously in order to find the magnetization of each plane at a temperature T and field h, from which we will obtain the magnetization of the entire film or multilayer. We therefore need to minimize

$$E = \sum_{d=1}^{D} [m_d - f(m_{d-1}, m_d, m_{d+1})]^2 = 0 \ . \tag{8}$$

This is done numerically by iterating all plane magnetizations by one of three possible changes: $+\delta$, 0, or $-\delta$, at the same time and checking which set of changes leads to the minimum of equation 8. This means that for D planes, D equations of state need to be solved at the same time, and each step towards the solution contains 3^D possibilities, which are all considered at each temperature step.

The accuracy of the solution of Eq. 4 depends on the step size δ and the value of E. In our simulations we vary the magnetization of each plane by $\delta = 10^{-5}\,|S|$ and require that $E \leq 10^{-6}$ is satisfied. This provides a very high resolution for the magnetization values and a high accuracy for the solution of the equations of state.

139   Using this procedure we simulate $M(T)$ curves for films with various thicknesses (D),
140 inter-plane (J^*), and inter-layer (J_{IEC}) exchange constants.

III.   RESULTS AND DISCUSSION

142   We calculated the plane magnetization of systems with $D = 1$ to 11, considering free films,
143 i.e., with $J_{\text{IEC}} = 0$. For systems with even number of planes, all magnetization contributions
144 are canceled out because the system is fully symmetric. For odd number of planes, however,
145 there is one uncompensated plane, which results in a non-zero magnetization of the system,
146 as expected according to Néel[33]. As will be seen later, however, the net magnetization is
147 not equal to the magnetization of any single uncompensated plane.

148   Figure 2(a) shows the net film magnetization $M(T)$ (solid lines) and the average absolute
149 value of plane magnetization $|m(T)|$ (dashed lines) of systems with odd number of planes
150 as a function of temperature. For the simplest system with one plane $(D = 1)$, there is
151 no inter-plane exchange and the system represents a typical MFA Ising ferromagnet with
152 ordering temperature $T_{\text{N}} = 150$ K. With increasing D, the ordering temperature increases
153 monotonically and approaches saturation after a few planes (see Fig. 2b), following Eq. 6.
154 For the system with $D = 11$ the ordering occurs at $T_{\text{N}}(11) = 0.983\,T_{\text{N}}(\infty)$.

155   This behavior of the ordering temperature is very similar to that of Heisenberg-type
156 ferromagnetic EuO films[5,22], and comparable to experimental observations in CoO/SiO_2
157 multilayers[11,12] and CoO/MgO and NiO/MgO superlattices[10]. The experimental values for
158 the ordering temperature of CoO with a thickness of 6 and 10 atomic planes in Ref.[10] were
159 255(5) K and 275(5) K, respectively, which is in very good agreement with the MFA predicted
160 values of $0.95\,T_{\text{N}}(\infty) \approx 270$ K and $0.98\,T_{\text{N}}(\infty) \approx 280$ K, for the corresponding thicknesses
161 (considering that the bulk value of that sample was 285 K). The monotonic increase of T_{N}
162 differs, however, from that of metallic FM films, where the Curie temperature sometimes
163 exceeds the bulk value due to the effect of surface electronic states[34–37], which marks a clear
164 distinction between metallic and oxide magnets.

165   Figure 2 further shows that with increasing thickness the shape of the $M(T)$ curve de-
166 parts strongly from the Brillouin-like shape of $D = 1$ and the difference between net film
167 magnetization $M(T)$ and average absolute plane magnetization grows surprisingly large (up
168 to 40% for $D = 11$ at $T = 3T_{\text{N}}/4$), due to the different magnetization of different planes.

169 As an example, for $D = 11$ the magnetization starts at a plateau for low temperature and
170 then decreases in a nearly linear fashion with increasing temperature, until it reaches T_N.

171   The changes in $M(T)$ become increasingly smaller with increasing D and show no signif-
172 icant changes for $D \geq 7$. This becomes clear if we compare the normalized $M(T)$ curves of
173 $D = 7$, 9, and 11, which have the same shape (see Fig. 2c). The evolution of $M(T)$ with D
174 is comparable to the evolution of the ordering temperature, which approaches saturation for
175 $D \geq 7$. This means that if we keep increasing D the $M(T)$ curve will not change further,
176 and the ordering temperature will eventually reach the bulk value.

177   While it may seem counterintuitive that the thinnest film behaves most like a mean field
178 magnet [with a Brillouin-function-like $M(T)$], this is due to a combination of finite size
179 effects plus the fact that this is an AFM where the magnetization of almost all planes is
180 compensated. The effect of finite-size is further investigated by observing the individual
181 plane magnetizations. Figure 3 shows the plane magnetization for systems with $D = 4$, 5,
182 10, and 11 as a function of temperature. As seen in the figure, the plane magnetization at
183 low temperature ($T \leq 0.4\ T_N$) is saturated for all planes, but for intermediate temperatures
184 ($0.4\ T_N \leq T \leq 1.0\ T_N$) it differs strongly between surface and core planes. The surface
185 planes have the weakest magnetization because they have a smaller number of interactions
186 compared to the core of the film. The planes directly below the surface also have reduced
187 magnetization because they are affected by the weaker magnetization of the outer planes.
188 Planes which are 2 or more monolayers below the surface also exhibit some differences, which
189 are however increasingly small. Similar magnetization profiles have been seen for antiferro-
190 magnetic Heisenberg EuTe(111) films, which exhibit strong finite-size effects, notably near
191 $T \approx 0.5\ T_N$[38].

192   For even-numbered systems (see Fig. 3a,c) all the plane magnetizations are canceled out
193 because the system is fully symmetric: equal number and equal absolute value of magne-
194 tization points in positive and negative direction, respectively. For odd-numbered systems,
195 however, (see Fig. 3b,d) the surface planes add to each other, the next two add to each
196 other and subtract from the top two, etc, generating the net film magnetization seen in Fig.
197 2. The net magnetization, notably, is not equal to the magnetization of any single uncom-
198 pensated plane, but is lower at all intermediate T. This is because the magnetization in the
199 positive direction, i.e., in the outer planes, changes differently with temperature compared
200 to the magnetization in the negative direction, i.e., in the inner planes, thus resulting in a

201 strongly reduced and modified $M(T)$ curve.

202 We now test the effects of the inter-plane exchange coupling J^* by simulating the system

203 with $D = 11$ for weaker ($\alpha = -0.5$) and stronger ($\alpha = -1.5$) coupling, and also consider

204 ferromagnetic cases with $\alpha = +0.5, +1.0$, and $+1.5$.

205 Figure 4 shows the comparison of $M(T)$ curves for the six different J^* values, (a) showing

206 the AFM and (b) the FM case. Considering first the AFM ($J^* < 0$) results, with decreasing

207 α-ratio the shape of the $M(T)$ curve changes and the curve becomes closer to the Brillouin-

208 like shape of the MFA ferromagnet seen in the $D = 1$ film. The reason for this behavior is

209 that with decreasing strength of J^*, the difference in energy between outer and inner planes

210 is reduced. In the limit of $J^* \to 0$, the system with $D = 11$ will behave as 11 decoupled

211 ferromagnets with an ordering temperature of the 2D system and a Brillouin-like $M(T)$

212 curve. In contrast, if we increase J^* the energy difference becomes larger: near surface

213 planes are increasingly weaker compared to the core planes and the $M(T)$ curve is modified

214 further.

215 These observations are also valid in the ferromagnetic case (Fig. 4b). The individual

216 plane magnetizations $m(T)$ (see inset to Fig. 4b) of a ferromagnetic film with $D = 11$

217 (with $\alpha = 1$) are exactly the same as the individual plane magnetizations $|m(T)|$ of the

218 AFM system shown in Fig. 3d. The ordering temperature of the FM is also the same

219 as in the AFM case, but since all plane magnetizations are positive, the shape of the net

220 magnetization $M(T)$ for $D = 11$ is only very slightly modified from the Brillouin form of

221 the $D = 1$ limit, in contrast to the case of AFM systems, and it is not strongly affected by

222 the α-ratio.

223 In the next step, we simulate multilayers of antiferromagnetic films each with $D = 11$

224 separated by non-magnetic layers by using a single $D = 11$ film and turning on an inter-layer

225 exchange coupling J_{IEC}, as shown in Fig. 1, and investigate its effect on the behavior of

226 the system. We assume that the IEC only acts on the surface planes, consistent with the

227 assumption throughout this paper of nearest neighbor exchange only, and with the nature

228 of the superexchange coupling of MO AFM's given the insulating nature of the MO layers.

229 We test its effects for $J_{\mathrm{IEC}} = 0.2\,J$ and $0.4\,J$, keeping $\alpha = -1$ for this set of simulations.

230 Figure 5 shows the net magnetization $M(T)$ as a function of the reduced temperature.

231 The black solid line shows $M(T)$ of the uncoupled film ($J_{\mathrm{IEC}} = 0$). The ordering tem-

232 perature does not change with increasing interaction energy, but the shape of the $M(T)$

curve changes markedly. Positive coupling between films increases the magnetization of the surface planes and reverses the effects of finite-size discussed above. In fact, if we consider the, unrealistic, limit of $J_{\mathrm{IEC}} = |z^*J^*|$, the periodic boundary condition is complete and finite-size effects disappear: all planes have exactly the same magnetization and there is no distinction between surface and film core because all planes have the same number of bonds with the same bond strength, which corresponds to the case of $D \to \infty$.

For negative J_{IEC} the exact same effect occurs; the near-surface magnetic moments are enhanced. For this calculation we used two films instead of one, and coupled the bottom plane of the first to the top plane of the second, because the negative IEC doubles the unit cell of the system. In this case the net magnetization of each film is antiparallel to that of its two neighboring films in the multilayer (data not shown), resulting in a zero magnetization of the multilayer, as seen experimentally for CoO/Al-ZnO multilayers[19].

For systems with even number of atomic planes, the effect of IEC (whether positive or negative) is the same, i.e., the magnetic moment near the surface at intermediate temperatures is enhanced. In this case, positive or negative IEC affects the direction of individual planes at the top and bottom of each layer, but the net magnetization of each film and in turn of the multilayer, however, is always zero because all individual plane magnetizations cancel each other out.

In addition to IEC, an external field can influence the ordering of an AFM film or multilayer. When we apply an external field h on the AFM films, the shape of the $M(T)$ curve is drastically changed and the ordering is strongly affected: the onset of magnetization at T_{N}, which remains unchanged, becomes increasingly smeared with stronger h (see inset to Fig. 5) due to paramagnetic effects above T_{N}. The presence of the external field, which acts upon all planes equally, increases the magnetization of odd-numbered planes (which have positive m), and decreases that of the even-numbered planes (which have negative m). Considering that the outer planes have weaker coupling to the inner of the film, they are more susceptible to the external field. The magnetic moment of the surface planes thus increases more, compared to that of the core planes. This change in the system corresponds to a reversing of the finite-size effects discussed above.

We continue by suggesting how our findings may be observed experimentally by comparing the net magnetization $M(T)$ of AFM films to the average absolute plane magnetization. The $M(T)$ curves shown in this paper represent theoretical experiments, where the vectorial

10

sum of the plane magnetizations is projected onto a measurement axis, like in a magnetome-
ter with small external fields. In other experiments, however, such as neutron diffraction, the
magnetic intensity is the average of the absolute plane magnetization $M_{\text{neutron}}(T) = |m(T)|$.
Fig. 2 showed that $M(T) \neq |m(T)|$, therefore a comparison of neutron diffraction intensity
and low applied field magnetometry $M(T)$ should show a difference for thin film AFM's
(Note that it is important that the magnetometry not be dominated by ferromagnetic im-
purities or second phases, or by the usual paramagnetic AFM contribution). In fact, this was
seen in CoO multilayers[19], which exhibited a somewhat different temperature dependence
in $M(T)$ measured in a magnetometer and the normalized neutron diffraction data, most
visible near $T = 0.5\,T_{\text{N}}$. Such a comparison can therefore be used to estimate the finite-size
effects including surfaces and grain boundaries in metal oxide AFM films and multilayers
and probe the extent to which surface magnetization is reduced in such low-dimensional
oxide antiferromagnets. Most importantly, the inequality $M(T) \leq |m(T)|$ is valid for any
AFM film regardless of the interaction parameters in the system. For any set of interaction
strengths $J > 0$ and $J^* < 0$ the net magnetization of an AFM film will always be lower than
the average plane magnetization, or the magnetization of any single uncompensated plane.

We note finally that the simulations in this work were done assuming perfect crystalline
planes with full atomic occupancy. In the case of defects or grain boundaries in real systems
the number of uncompensated spins increases drastically and may produce similar effects
as the ones found here. In addition, however, uncoupled spins, e.g. on rough surfaces or
corners, can exhibit *paramagnetic* behavior which can strongly influence the $M(T)$ curve of
the films in the presence of an external field.

IV.   CONCLUSIONS

We have simulated antiferromagnetic thin films with thicknesses of up to 11 crystalline
planes using mean-field approximation. Our study showed that films with an even number of
planes have zero magnetization at all temperatures, whereas odd-numbered systems exhibit
ferromagnetism due to unequal magnetization of near surface layers, where the net magne-
tization of the film is lower than that of any single uncompensated plane at intermediate
temperatures. With increasing film thickness the Néel temperature increases monotonically
and reaches the bulk value after a few planes, while the form of the $M(T)$ curve is dramat-

ically changed due to finite-size effects at near-surface planes which dominate AFM films despite having little effect on FM films due to compensation. The difference between near-surface magnetization and the core of the film changes strongly with inter-plane coupling: with smaller J^* it becomes smaller because the energy difference between outer and inner planes becomes lower, and vice versa. We also found that turning on a positive inter-layer exchange coupling inhibits these finite-size effects and promotes ferromagnetism in odd numbered systems by increasing the surface magnetization, whereas negative IEC results in zero net magnetization due to full cancellation of magnetic moments in a multilayer. Finally, we showed how these effects can be observed experimentally by comparing temperature-dependent magnetization measurements and neutron diffraction experiments.

ACKNOWLEDGMENTS

[310] * Corresponding author. Email: charilaou@berkeley.edu

[311] [1] F. Aguilera-Granja and J. L. Morán-López, Solid State Commun. **74** No. 3, 155 (1990).

[312] [2] P. J. Jensen, H. Dreyssé, and K. H. Bennemann, Surf. Sci. **269/270**, 627 (1992).

[313] [3] O. Hjortstam, J. Trygg, J. M. Wills, B. Johansson, and O. Eriksson, Phys. Rev. B **53**, 9204

[314] (1996).

[315] [4] A. Ney, P. Poulopoulos, and K. Baberschke, Europhys. Lett., **54** (6), 820 (2001).

[316] [5] R. Rausch and W. Nolting, J. Phys.: Condens. Matter **21**, 376002 (2009).

[317] [6] J. J. Alonso and Julio F. Fernández, Phys. Rev. B **74**, 184416 (2006).

[318] [7] K. K. Pan, Phys. Rev. B **64**, 224401 (2001); Phys. Rev. B **71**, 134524 (2005); Physica A (in

[319] press) doi:10.1016/j.physa.2011.11.048.

[320] [8] H. T. Diep, Phys. Rev. B **43**, 8509 (1991).

[321] [9] M. Takano, T. Terashima, Y. Bando, and H. Ikeda, Appl. Phys. Lett. **51**, 205 (1987).

[322] [10] E. N. Abarra, K. Takano, F. Hellman, and A. E. Berkowitz, Phys. Rev. Lett. **77**, 3451 (1996).

[323] [11] T. Ambrose and C. L. Chien, Phys. Rev. Lett. **76**, 1743 (1996).

[324] [12] Y. J. Tang, D. J. Smith, B. L. Zink, F. Hellman, and A. E. Berkowitz, Phys. Rev. B **67**, 054408

[325] (2003).

[326] [13] W. H. Meiklejohn and C. P. Bean, Phys. Rev. **105**, 904 (1957).

[327] [14] M. N. Baibich, J. M. Broto, A. Fert, F. Nguyen van Dau, F. Petroff, P. Etienne, G. Creuzet,

[328] A. Friederich, and J. Chazelas, Phys. Rev. Lett. **61**, 2472 (1988).

[329] [15] C. G. Shull, W. A. Strauser, E. O. Wollan, Phys. Rev. **83**, 333 (1951).

[330] [16] J. Kanamori, Prog. Theor. Phys. (Japan) **17**, 177 (1957); **17**, 197 (1957).

[331] [17] W. L. Roth, Phys. Rev. **110**, 1333 (1958).

[332] [18] R. M. Cornell and U. Schwertmann, *The Iron Oxides* John Wiley & Sons Ltd (2003).

[333] [19] H.-J Lee, C. Bordel, J. Karel, D. W. Cooke, M. Charilaou, and F. Hellman, Phys. Rev. Lett.

[334] **110**, 087206 (2013).

[335] [20] K. Binder and P. C. Hohenberg, Phys. Rev. B **9**, 2194 (1974).

[336] [21] D. P. Landau and K. Binder, J. Magn. Magn. Mater. **104–107**, 841 (1992).

[337] [22] W. Nolting and C. Santos, Physica B **321**, 189 (2002).

[338] [23] Y. Laosiritaworn, J. Poulter, and J. B. Staunton, Phys. Rev. B **70**, 104413 (2004).

13

[339] [24] N. M. Mermin and H. Wagner, Phys. Rev. Lett. **17**, 1133 (1966).

[340] [25] A. Gelfert and W. Nolting, Phys. Stat. Sol. B 217, 805 (2000).

[341] [26] R. Agra, F. van Wijland, and E. Trizac, Eur. J. Phys. **27**, 407 (2006).

[342] [27] M. Charilaou, K. K. Sahu, A. U. Gehring, J. F. Löffler, Phys. Rev. B **86**, 104415 (2012).

[343] [28] M. B. Salamon, Phys. Rev. B **2**, 214 (1970).

[344] [29] S. Zhang and G. Zhang, J. Appl. Phys. **75**, 6685 (1994).

[345] [30] V. Staemmler, K. Fink, Phys. Chem. **278**, 79 (2002).

[346] [31] W. Haubenreisser, W. Brodkorb, A. Corciovei, G. Costache, phys. stat. sol. **53**, 9 (1972).

[347] [32] P. M. Levy, S. Maekawa, P. Bruno, Phys. Rev. B **58**, 5588 (1998).

[348] [33] L. Néel, C. R. Acad. Sc., **203**, 304 (1936).

[349] [34] M. Stampanoni, A. Vaterlaus, M. Aeschlimann, and F. Meier, Phys. Rev. Lett. **59**, 2483 (1987).

[350] [35] M. Stampanoni, Appl. Phys. A **49**, 449 (1989).

[351] [36] C. Liu and S. D. Bader, J. Appl. Phys. **67**, 5758 (1990).

[352] [37] Y. Li and K. Baberschke, Phys. Rev. Lett. **68**, 1208 (1992).

[353] [38] E. Schierle, E. Weschke, A. Gottberg, W. Söllinger, W. Heiss, G. Springholz, and G. Kaindl,

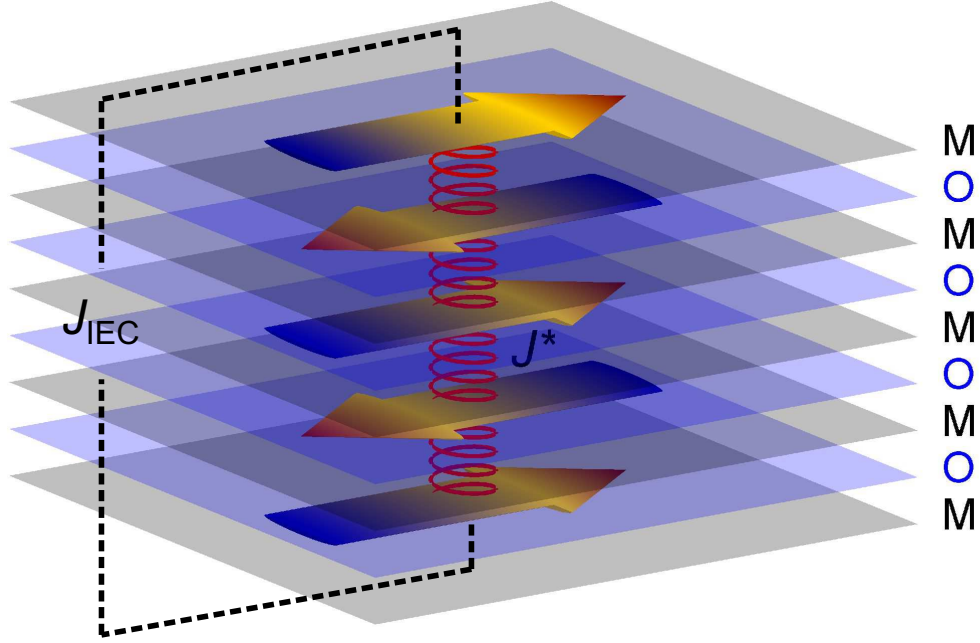[354] Phys. Rev. Lett. **101**, 267202 (2008).

FIGURES

FIG. 1. Illustration of the layered structure of an antiferromagnetic film with 5 planes. Alternating (111) planes of the NaCl structure are completely filled with metal ions (M) and oxygen (O) consecutively. The arrows inside the M planes indicate the alternating direction of the plane magnetization and the red springs correspond to the inter-plane exchange coupling J^*. The simulation of multilayers is performed by coupling the top and the bottom planes as indicated by the J_{IEC} bond.
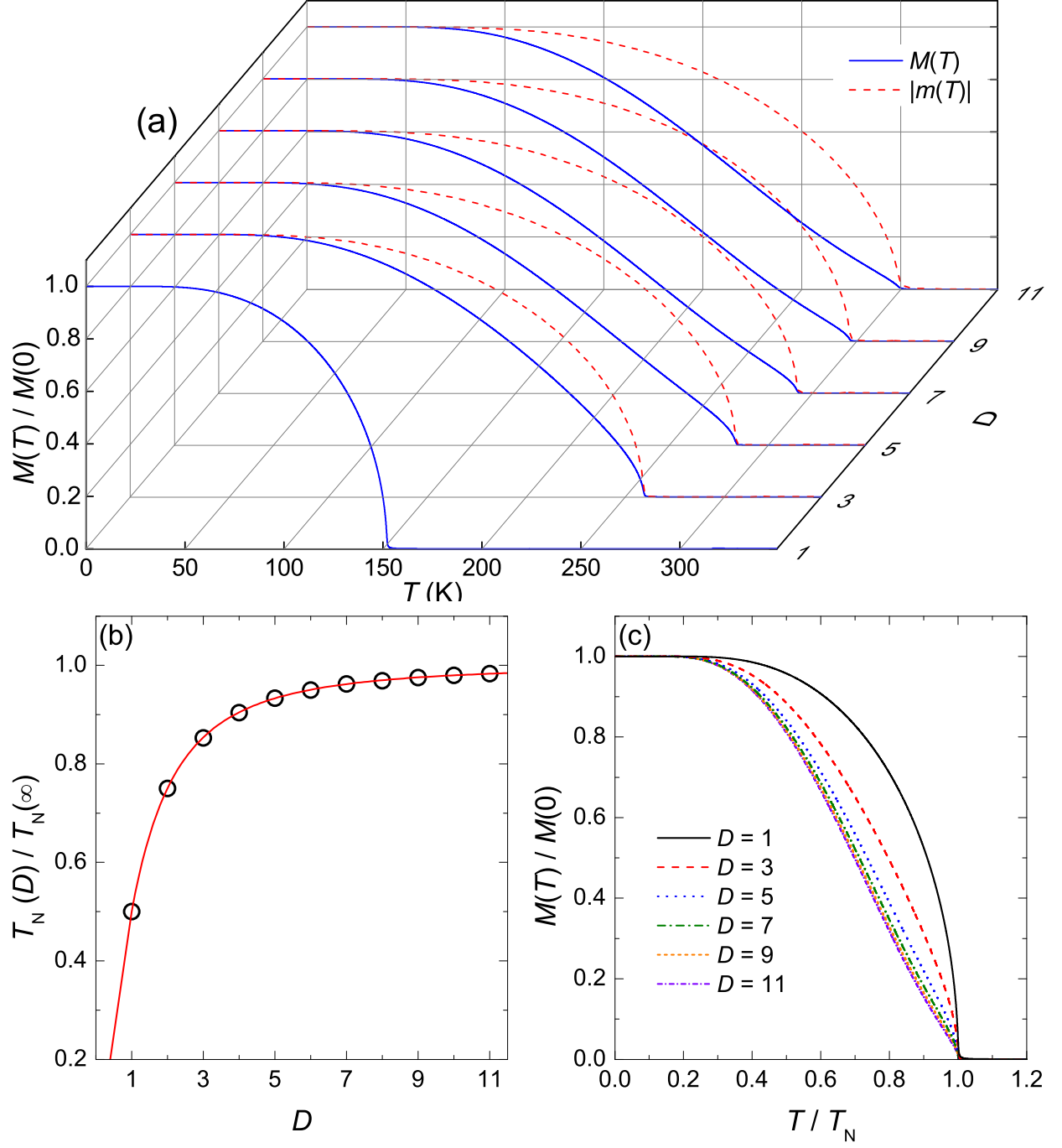
FIG. 2. (a) Magnetization of systems with odd number of monolayers as a function of temperature. Solid lines correspond to the net film magnetization $M(T)$ and dashed lines correspond to the average absolute plane magnetization $|m(T)|$. (b) Evolution of the ordering temperature T_N as a function of D; the solid line corresponds to Eq. 6. (c) Normalized $M(T)$ curves as a function of T/T_N. With increasing D the $M(T)$ curve departs from the Brillouin-like shape and becomes nearly linear in the range $0.5 \leq T/T_N \leq 1.0$.

FIG. 3. Plane magnetization of the systems with (a) $D = 4$, (b) 5, (c) 10, and (d) 11 as a function of temperature. The surface planes [e.g. 1 and 4 or 5 in a) and c), and 1 and 10 or 11 in b) and d)] have weaker magnetization compared to the inner planes. For even number of monolayers the magnetization is fully symmetric ($m_{\text{odd}} = -m_{\text{even}}$) and the net sum $M(T)$ is zero (not shown), whereas for odd-numbered systems the surface magnetization is uncompensated and results in a net non-zero magnetization ($m_{\text{odd}} \neq -m_{\text{even}}$), shown as a solid lines marked $M(T)$ in the right panels. Note that $M(T)$ is lower than the magnetization of any single uncompensated plane at intermediate temperatures.
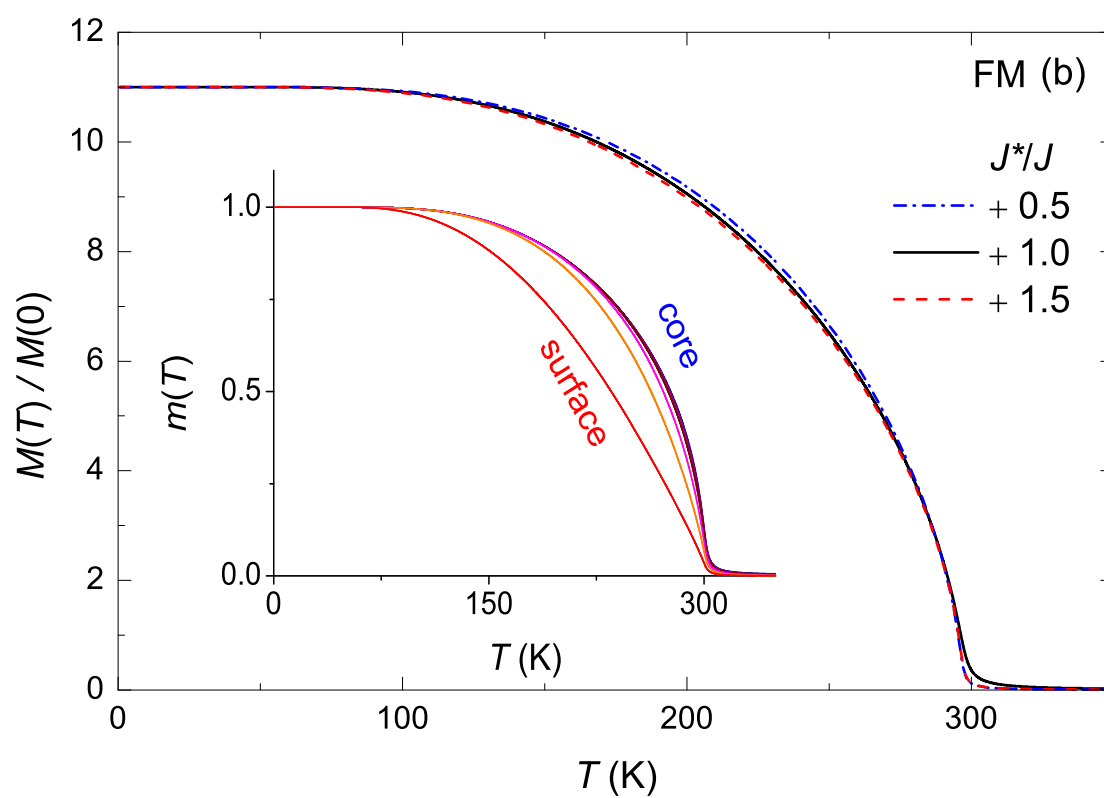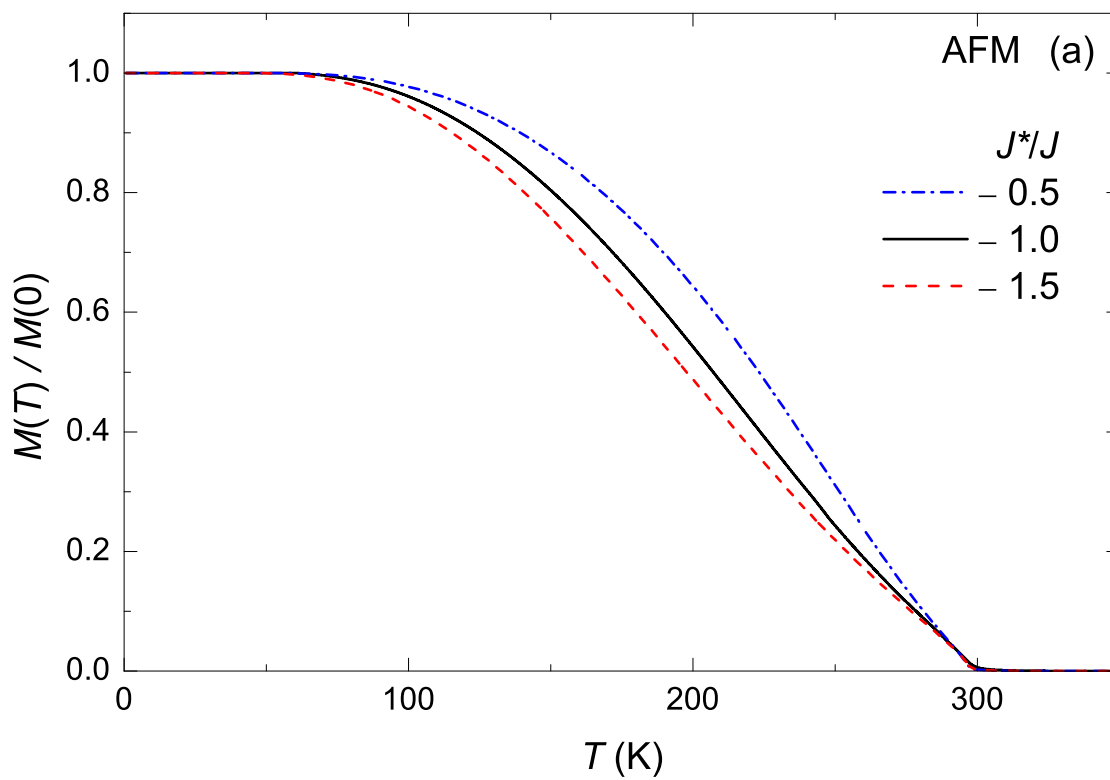
FIG. 4. Net magnetization of the system with $D = 11$ as a function of temperature. The three different calculations correspond to cases where $\alpha = J^*/J = -0.5$ (dash-dotted blue line), -1.0 (solid black line), and -1.5 (dashed red line) for the AFM case and $J^*/J = +0.5$, $+1.0$, and $+1.5$ for the FM case. The inset to (b) shows the magnetization of several important planes in the FM film. The near-surface magnetic moments in FM systems are reduced, in exactly the same manner as in the AFM case.
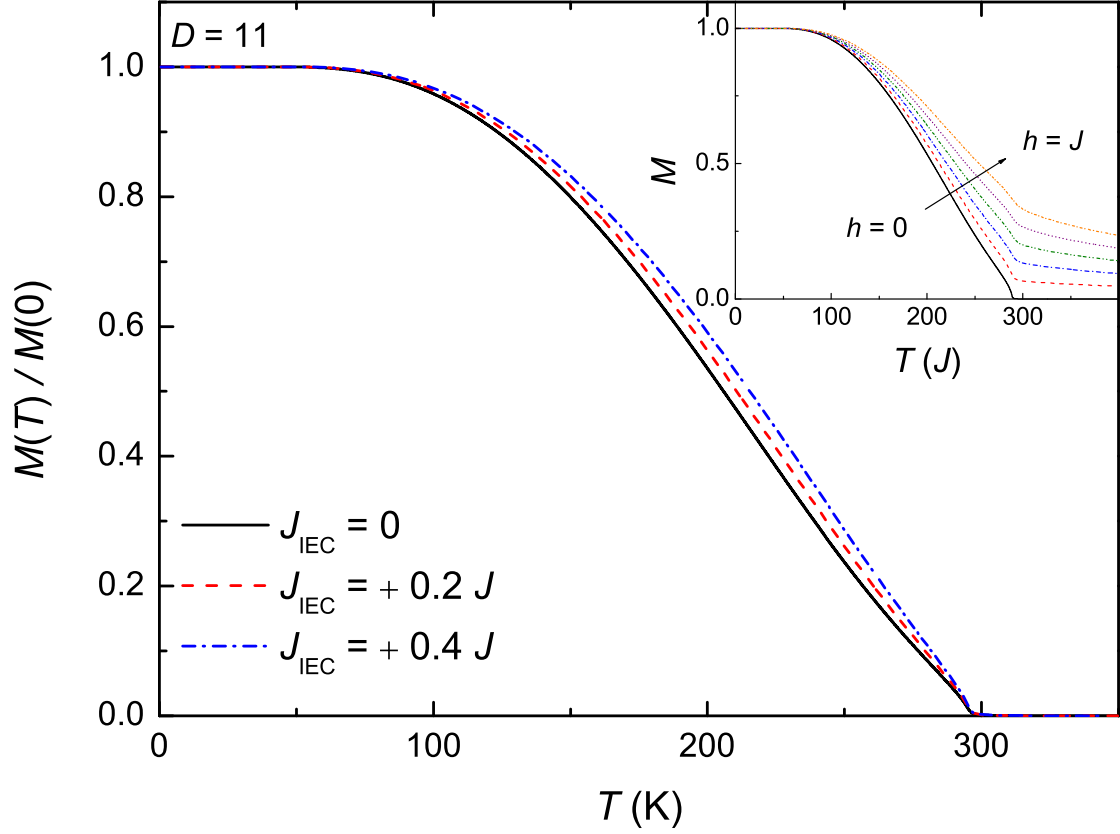
FIG. 5. Net magnetization per film for systems with $D = 11$ and $J^* = -J$ as a function of temperature with different strengths of IEC. With increasing IEC strength $M(T)$ is enhanced; this is because the IEC acts on the surface planes, which in turn affect the near-surface planes. The inset shows the effect of the external field h on the $M(T)$ curve.